Title
The effect of large-scale model time step and multiscale coupling frequency on cloud climatology, vertical structure, and rainfall extremes in a superparameterized GCM

Journal
Journal of Advances in Modeling Earth Systems, 7(4)

ISSN
1942-2466

Authors
Yu, Sungduk
Pritchard, Michael S

Publication Date
2015-12-01

DOI
10.1002/2015ms000493

AGU PUBLICATIONS

Journal of Advances in Modeling Earth Systems

RESEARCH ARTICLE

10.1002/2015MS000493

Key Points:
- Scale coupling frequency is a useful parameter impacting climatology in superparameterized GCMs
- Cloud condensate reduces and tropical rainfall extremes increase with high scale coupling frequency
- Changes in deep convective organization seem to be the main cause of climatological sensitivity

Supporting Information:
- Supporting Information S1

Correspondence to:
S. Yu,
sungduk@uci.edu

Citation:
Yu, S., and M. S. Pritchard (2015), The effect of large-scale model time step and multiscale coupling frequency on cloud climatology, vertical structure, and rainfall extremes in a superparameterized GCM, *J. Adv. Model. Earth Syst.*, *7*, 1977–1996, doi:10.1002/2015MS000493.

Received 5 JUN 2015
Accepted 19 OCT 2015
Accepted article online 26 OCT 2015
Published online 17 DEC 2015

The effect of large-scale model time step and multiscale coupling frequency on cloud climatology, vertical structure, and rainfall extremes in a superparameterized GCM

Sungduk Yu[1] and Michael S. Pritchard[1]

[1]Department of Earth System Sciences, University of California, Irvine, California, USA

Abstract The effect of global climate model (GCM) time step—which also controls how frequently global and embedded cloud resolving scales are coupled—is examined in the Superparameterized Community Atmosphere Model ver 3.0. Systematic bias reductions of time-mean shortwave cloud forcing (~10 W/m^2) and longwave cloud forcing (~5 W/m^2) occur as scale coupling frequency increases, but with systematically increasing rainfall variance and extremes throughout the tropics. An overarching change in the vertical structure of deep tropical convection, favoring more bottom-heavy deep convection as a global model time step is reduced may help orchestrate these responses. The weak temperature gradient approximation is more faithfully satisfied when a high scale coupling frequency (a short global model time step) is used. These findings are distinct from the global model time step sensitivities of conventionally parameterized GCMs and have implications for understanding emergent behaviors of multiscale deep convective organization in superparameterized GCMs. The results may also be useful for helping to tune them.

1. Introduction

It is well known that in global climate models (GCMs) using cumulus parameterizations, key aspects of the simulation performance can depend sensitively on the GCM time step. The partitioning between precipitation determined by large-scale dynamics versus cumulus parameterization is sensitive to model time step, with implications for rainfall extremes [*Williamson*, 2008; *Mishra et al.*, 2008; *Mishra and Sahany*, 2011]. In addition, the geographic structure of zonal mean precipitation structures can also be sensitive to the GCM time step, even switching between either single-intertropical or double-intertropical convergence zone states depending on the GCM time step and dynamical core used in aqua-planet simulations with the Community Atmosphere Model ver 3.0 (CAM3) [*Williamson*, 2008; *Mishra et al.*, 2008; *Li et al.*, 2011] and its preceding version [*Williamson and Olson*, 2003]. These studies also found tropical mean precipitation can also be somewhat sensitive to the GCM time step with mean precipitation rate increasing with a shorter time step.

Williamson [2013] argued many of these sensitivities may be a manifestation of deep and shallow convective parameterization schemes failing to effectively eliminate moist instability by vertical redistribution and associated condensation when the adjustment timescales assumed in convective parameterizations are longer than a GCM time step. Consistent with this view, they showed convective precipitation decreases with a reduced GCM time step in a high-resolution aqua-planet version of CAM4. One way to think of their physical idea is that when convective parameterizations do not have enough time to remove a substantial amount of moist instability in between GCM time steps, a feedback with the large-scale circulation may occur, either because of differences in the latent heating profile leading to different circulations and increased moisture convergence (and gross moist stability) or because it may be easier for the large-scale precipitation scheme to convert moisture convergence to precipitation than for a convection scheme (or is realistic in a convecting environment). These sorts of mechanisms can result in coarse grid-scale overturning, generating heavy precipitation events, and so-called "grid-point storms"—unrealistically intense, short-lived precipitation events occurring at the GCM grid scale.

It is unknown whether superparameterized (SP) GCMs—in which cumulus parameterizations are replaced with cyclic two-dimensional cloud resolving models (CRMs) in each grid column—exhibit similar sensitivities to the time step of the exterior model, namely the GCM. This is the problem we will address.

As a null hypothesis (H0), it is logical to predict that the exterior model time step sensitivities of SPGCMs should be much less striking than normal GCMs since SPGCMs do not rely on rigid assumptions about

convective instability depletion timescales, unlike most conventional cumulus parameterizations. Thus theoretically, convective instabilities exposed to embedded CRMs should always efficiently be removed as they develop, leading to expectations of reduced grid-point storm sensitivities in SPGCMs (D. Randall, personal communication, 2014). Hypothesis H0 predicts SPGCMs should be mostly *insensitive* to large-scale model time step, unlike normal GCMs.

However, there are also logical reasons to think the global model time step may matter to SPGCM simulations in new and important ways. After all, the scale separation between GCM and CRM intrinsic to SP models is more artificial than natural, and information is only allowed to be exchanged between the two resolved scales at each GCM time step. That is, the global model time step may have a bigger impact in an SPGCM than it does in a conventional GCM—it is also the primary control on the *scale coupling frequency*, f_{scale}. In this capacity, the global model time step may affect the simulations of SPGCMs in ways that are unfamiliar, and to emphasize this point we will refer to the global model time step as f_{scale} in subsequent discussion.

Specifically, we propose an alternative working hypothesis (H1) (B. Mapes, personal communication, 2014) based on recent ideas about *convective throttling* in SPGCM simulations by *Pritchard et al*. [2014] (PBD14 hereafter). PBD14 argued that the number of grid columns in an SPGCM's embedded CRMs may artificially limit the efficiency of deep convective mixing in a way that has important consequences for simulated cloud climatology, such as overly strong shortwave cloud forcing from too dense liquid clouds when small CRMs are used. This view is consistent with a variety of quasilinear biases observed to develop as the horizontal extent and number of grid columns in embedded CRMs are reduced.

The implications of these physics might imply scale coupling sensitivities in SPGCMs. Since the convective throttling effect is purely local and internal to the embedded CRM in each GCM grid cell, it is natural to wonder if it may be buffered through exposure to large-scale dynamics—which have the capacity to remove CRM-extent-throttled instability through interactions with large-scale wave modes and large-scale advection at the GCM scale. Thus our alternative convective throttling hypothesis (H1) predicts more frequent scaling coupling should unwind the mean state cloud biases that develop with reduced CRM extent. That is, hypothesis H1 predicts SPGCMs should be *sensitive* to decreased global model time steps in a fashion that is reverse to the sensitivities previously documented as a function of CRM extent in PBD14.

Beyond H0 and H1, there are other exploratory hypotheses that could be conceived for how—especially through its effect on scale coupling frequency—the GCM model time step might impact the vertical diabatic heating profile or mean state climatology of clouds in superparameterized models. In short, it is not obvious how to predict what the impact of scale coupling on SP simulations should be, or how default GCM model time step settings may have constrained previous SP simulations. Clearly, systematic testing is needed—primarily as a strategy to inform better understanding of the physical essence of emergent multiscale organized convection physics in SPGCMs. A secondary practical goal is to see if the scale coupling frequency is a useful tuning knob in SPGCMs that might help improve the fidelity of climate simulations with explicit convection.

This paper documents the effects of global model time step (and consequently scale coupling frequency f_{scale}) on the simulated climate in the Superparameterized Community Atmospheric Model 3. Several interesting sensitivities, many of which are monotonic to f_{scale}, are discovered. Section 2 describes the model and the experimental designs. Section 3 shows the major findings. Section 4 contains further discussion and some ideas for future work. Section 5 concludes.

2. Methodology

2.1. Model Description

The Superparameterized Community Atmospheric Model ver 3.0 (SPCAM3) is used for all simulations in this study. Its exterior large-scale model is a version of Community Atmospheric Model 3.0 that uses a semi-Lagrangian dynamical core with T42 spectral resolution and 30 vertical levels. Over eight thousand 2-D CRMs with 4 km horizontal grid spacing are embedded to replace deep and shallow cloud and boundary layer turbulence parameterizations in each grid cell (superparameterization) [*Grabowski and Smolarkiewicz*, 1999; *Grabowski*, 2001]. The embedded CRM is a legacy version of the System of Atmospheric Model

Table 1. The Summary of SPCAM Simulations Performed in This Study

Simulation	dtime600	dtime900	dtime1800	dtime3600
Time step (s)	600	900	1800	3600
f_{scale} (1/h)	6	4	2	1

[*Khairoutdinov and Randall*, 2003]. This essence of this version of SPCAM3 has been widely used by *Khairoutdinov et al*. [2005], *Khairoutdinov et al*. [2008], *Benedict and Randall* [2009], and *Thayer-Calder and Randall* [2009]. We use a somewhat unusual "micro-CRM (8 × 1 column)" configuration of superparameterization used by PBD14, in which the micro-CRM is one quarter the size of the conventional CRM setup of 32 × 1 columns. This is chosen for two practical reasons. First, it usefully enforces a baseline model configuration that is already known to be highly "throttled," with results that can be directly compared to that study. We view this as helpful for testing the expectation of H1: that increasing f_{scale} could decrease the effect of throttled deep convection due to a limited CRM domain extent. Second, it is also a useful model configuration for computational efficiency, enabling 4 times faster simulations in a computationally demanding GCM. The specific code version of SPCAM3 that was used for integrations is archived by the Center for Multiscale Modeling for Atmospheric Processes at: https://svn.sdsc.edu/repo/cmmap/cam3_sp/branches/pritchard (rev. 304).

2.2. Experimental Design

Our experiment includes four cases with different values of the host GCM (CAM3) model time step, and hence f_{scale}. The control case uses a GCM time step of 1800 s, which has been a convention of SPCAM3 simulations at T42 resolution [e.g., *Khairoutdinov et al*., 2005; *Wyant et al*., 2006; *Khairoutdinov et al*., 2008; *Benedict and Randall*, 2009; *Pritchard et al*., 2011; *Goswami et al*., 2011; *Pritchard et al*., 2014]. The experimental cases have GCM time steps of 600, 900, and 3600 s (f_{scale} is higher with a smaller time step). Table 1 summarizes the simulations performed. In all cases, regardless of global model time step, the CRM time step is 20 s, and the radiative transfer calculation is generally done every 900 s. The one exception is the 600 s time step case, in which the radiative transfer calculation is done every 600 s due to technical eccentricities of the SPCAM3 code. The simulation period is from September 1980 to December 1990. The first 4 months of spin-up period are discarded, and a complete decade of output (1981–1990) is used for climatological analysis. Sea surface temperature is prescribed based on time-varying monthly mean observed sea surface temperatures [*Hurrell et al*., 2008].

3. Results

3.1. Cloud Forcing Bias Reduction With a Higher f_{scale}

Figure 1 shows zonally averaged annual top-of-atmosphere cloud forcings of model simulations and satellite observation. In all simulations (thin lines), clouds are optically too thick, especially in the shortwave compared to CERES-EBAF ed 2.8 [*Loeb et al*., 2009] observations (thick lines). Inconsistent with hypothesis H0, several sensitivities to f_{scale} are immediately apparent. Interestingly, both the zonally averaged annual shortwave cloud forcing bias (SWCF; blue) and longwave cloud forcing bias (LWCF; red) improve with a higher f_{scale}. This suggests that f_{scale} can be a useful tuning knob for slightly reducing cloud radiative effect biases in SP models, with a reduced GCM time step producing improved cloud climatology. While the responses of zonally averaged SWCF and LWCF are both monotonic to f_{scale}, the magnitude of the SWCF response is about twice as large as that of the LWCF response. This suggests low, liquid clouds respond more sensitively to f_{scale} than high, ice clouds do.

It is natural to wonder whether the reduction in cloud radiative forcing is simply driven by a fundamental reduction in precipitation, or deep convection in general. Zonally averaged annual precipitation (Figure 2) shows that this is not the case because the zonally averaged annual precipitation both increases and decreases with increasing f_{scale} in the tropics, where the zonally averaged annual cloud radiative forcings systematically decrease with increasing f_{scale}. The precipitation response to f_{scale} is clearly less systematic and less sensitive (at least for the 600–1800 s time step regime) than the cloud radiative response.

We hone in on the SWCF responses, since they are found to be the most significant sensitivity to f_{scale} (magnitude of $\sim$10 W/m^2). Figure 3a shows their global structure. This demonstrates that the zonal mean annual SWCF response is predominantly from the equatorial deep convective regions. As we will discuss in section 3.4, this could be viewed as consistent with our working hypothesis H1, which predicts convective mixing

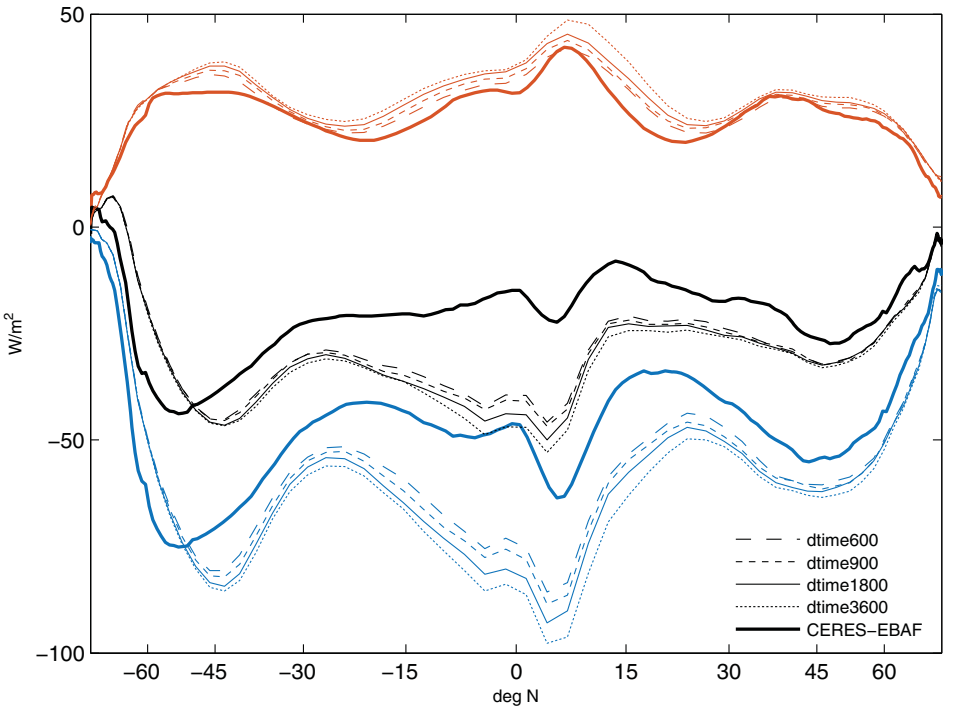

Figure 1. Zonally averaged annual mean net (black), shortwave (blue), and longwave (red) cloud forcing in SPCAM3 simulations (thin lines) and observation (thick solid lines).

efficiency is sensitive to f_{scale} due to the convective throttling effects. The sensitivity of SWCF to f_{scale} is geographically consistent with liquid water path (LWP) responses (Figure 3b), i.e., with increasing f_{scale}, SWCF reduces in regions of deep convection consistent with less liquid cloud in the same regions.

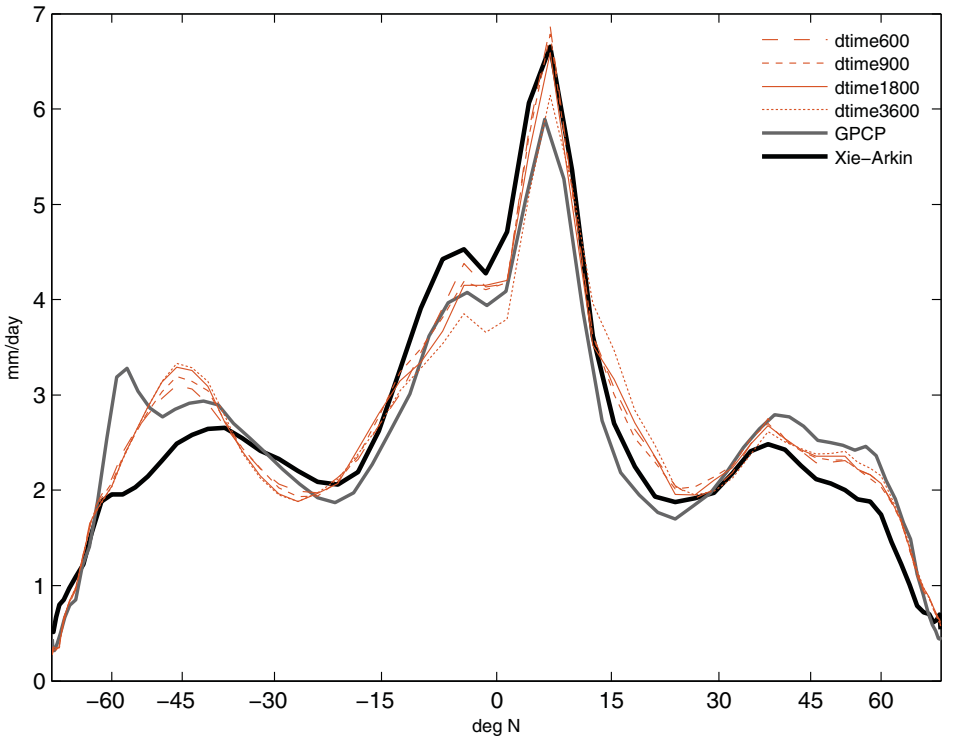

Figure 2. Zonally averaged annual mean precipitation rate in SPCAM3 simulations (thin lines) and observation (thick solid lines).

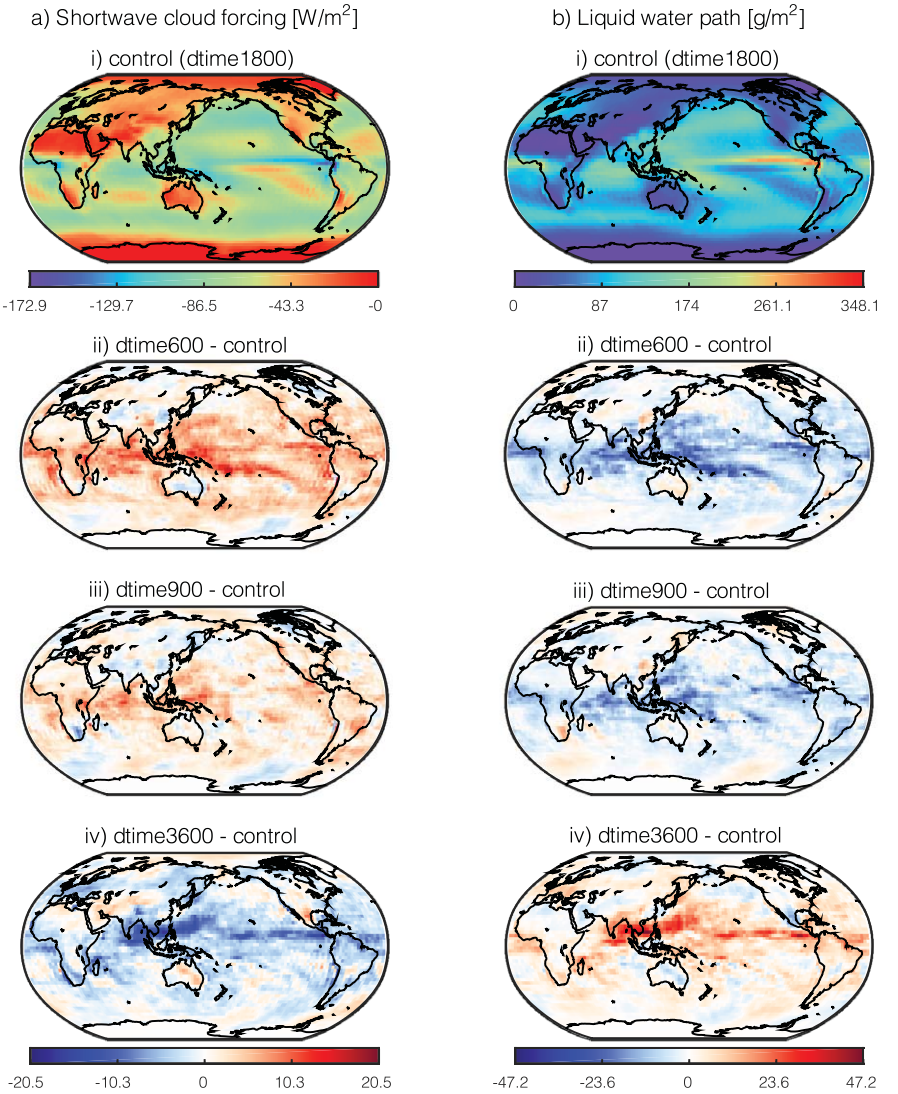

Figure 3. (a) Annual mean shortwave cloud forcing and (b) liquid water path from SPCAM3 simulations. (i) Control simulation and (ii–iv) experiment simulation anomalies against control simulation.

The LWCF response to f_{scale} is not expected from our working hypothesis (H1) because such a systematic response in LWCF was unseen in the CRM-domain restriction experiments of PBD14. We note that although the LWCF responses do show a systematic sensitivity to f_{scale}, the magnitude of this response is only half that of the SWCF sensitivity ($\sim$5 W/m^2), such that this is a secondary response. Figure 4a shows the global map of LWCF responses to f_{scale}. The LWCF responses are geographically more complex than the SWCF responses. The largest responses are still from the active convective regions—particularly Indo-Pacific Warm Pool region—as the SWCF responses are. But unlike the SWCF responses, the LWCF responses are not primarily concentrated in regions of the deepest tropical convection; there is an extratropical signal component that is more noticeable compared to the SWCF responses. Unsurprisingly, the LWCF responses are geographically consistent with ice water path (IWP) responses (Figure 4b), i.e., with increasing f_{scale} the LWCF responses weaken in many regions, consistent with less ice cloud, though many regional anomalies are apparent. Clearly, f_{scale} affects the mean condensate amount in SPCAM3.

The nature of the overall sensitivity to f_{scale} seems geographically distinct for the longest time step analyzed (3600 s). In this case, both SWCF and LWCF responses shift northward in the tropics, consistent with a bifurcation of the preferred mode of tropical mean state rainfall climatology (Figure 5). Such meridional shifts

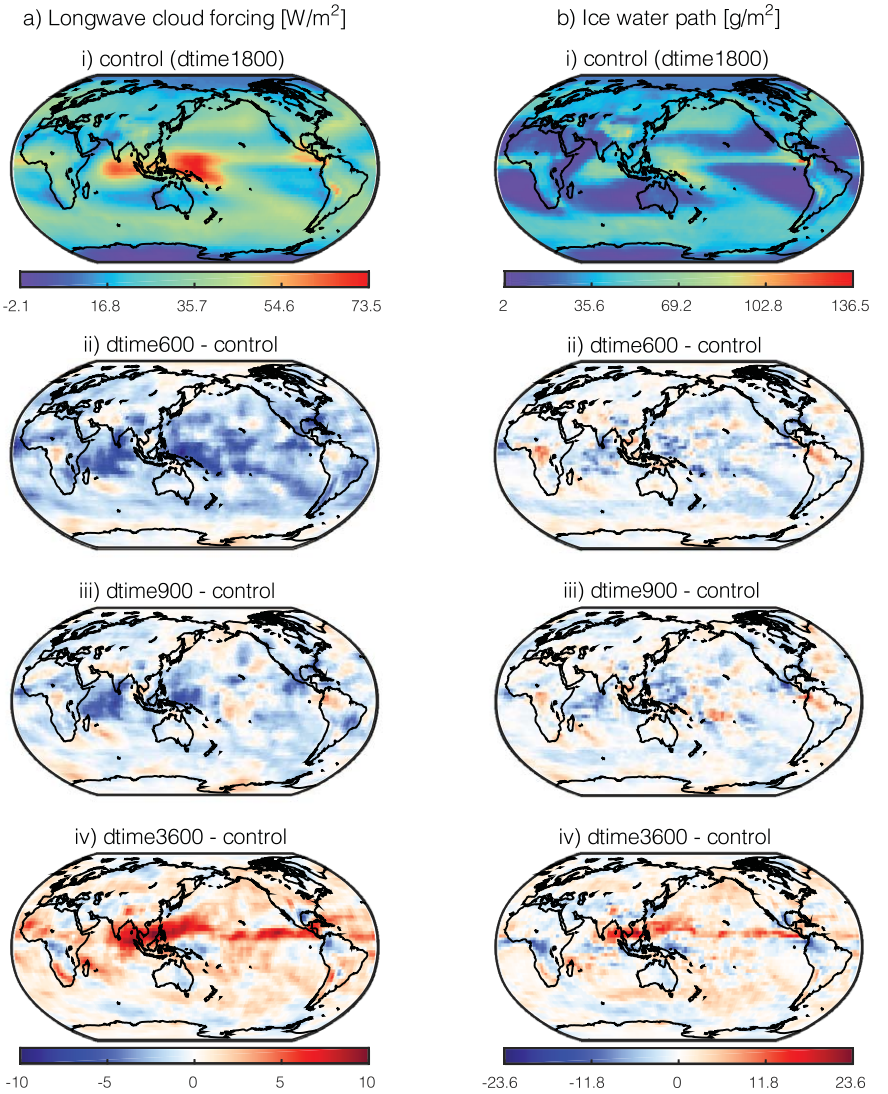

Figure 4. (a) Annual mean longwave cloud forcing and (b) ice water path from SPCAM3 simulations. (i) Control simulation and (ii–iv) experiment simulation anomalies against control simulation.

are not observed in the other tests, in which the geographic responses looks more scattered rather than a systematic shift. This contextual difference is useful to keep in mind.

3.2. Amplification of Tropical Rain Extremes With Increasing f_{scale}

An unexpected finding in our simulations is that the tail of the tropical precipitation rate distribution (viewed from the perspective of the logarithmically-binned rainfall distribution, following *Pendergrass and Hartmann* [2014a, 2014b]) intensifies as f_{scale} increases (Figures 6a and 6c). Interestingly, this does not occur in the extratropics, where the precipitation distribution is virtually insensitive to f_{scale} (Figures 6b and 6d). This is an unfavorable sensitivity, amplifying preexisting biases against daily observations from GPCP 1DD ver 1.2 [*Huffman et al*., 2001] and TRMM 3B42 ver 7 [*Huffman et al*., 2007]. This exacerbates the preexisting bias of an overly intense extreme rainfall tail when using the "micro-CRM" configuration of SPCAM3 as noted in PBD14. We acknowledge that current gridded estimates of surface precipitation derived from gauge-calibrated, IR-filled, microwave satellite-merged products do not produce convergence of extreme rainfall rate magnitudes on subpentad timescales [*Liu and Allan*, 2012], such that it is difficult to select between either GPCP 1DD ver 1.2 or TRMM 3B42 ver 7 as "truth" in this analysis. TRMM 3B42 ver 7 tends to produce better agreement with rain gauge measurements in the tropics [*Tan et al*., 2015] and incorporates

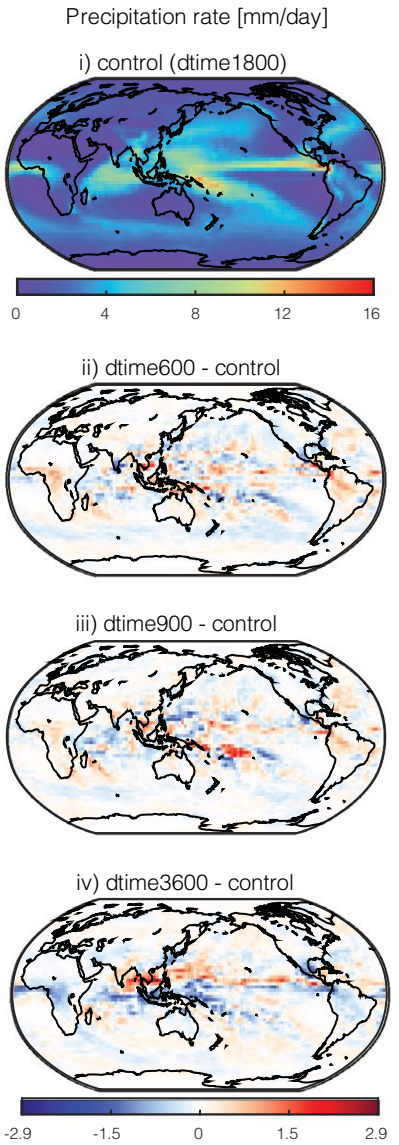

Figure 5. Annual mean precipitation rate from SPCAM3 simulations. (i) Control simulation and (ii–iv) anomalies against control simulation.

more microwave data streams than GPCP 1DD [*Rossow et al.*, 2013]. Accordingly, TRMM 3B42 ver 7 might be viewed as a more plausible baseline given raw microwave agreement with ground-based radar [*Wolff and Fisher*, 2009].

The precipitation distribution response to f_{scale} is mostly a shift of precipitation regimes from mid-precipitation to heavy-precipitation events in the tropics (Figures 6a and 6c). While the dry-rain frequency ($<$1 mm/d) is relatively insensitive to f_{scale}, the mid-rain band (1–50 mm/d) is suppressed and the heavy-rain band ($>$50 mm/d) boosts systematically with increasing f_{scale}. Whereas maps (Figure 5) of the geographic structure of the mean precipitation response to f_{scale} suggest a regional redistribution, maps (not shown) of the precipitation variance response to f_{scale} show a tropics-wide systematic response—e.g., boosting precipitation variance monotonically with f_{scale} throughout the climatologically active precipitation centers in the tropics. This suggests that the tropical precipitation tail responses are probably due to a shift in some fundamental character of tropical convection and not a systematic change in the mean rainfall rate.

Is the striking sensitivity of the tropical rainfall tail associated with amplification of a particular mode of equatorial wave variability? Zonal wavenumber-frequency power spectra [e.g., *Wheeler and Kiladis*, 1999] are shown to examine the equatorial wave response to f_{scale}. Figures 7a–7d show the log power of zonal wavenumber-frequency spectra of equatorially symmetric daily precipitation rate from 10°S to 10°N. Figures 7e–7g show the log ratios of responses of the experimental simulations to the control simulation.

No obvious mode of variability has responded to f_{scale}. Rather, the first-order response to f_{scale} is a shift of spectral power to higher frequencies at all zonal wavenumbers as f_{scale} increases; this is not as obvious in precipitation at low f_{scale} simulation (3600 s time step) whose spectral power decreases through a whole domain with a high frequency domain showing the largest reduction. There is a subtle sign that the moist Kelvin wave modes speed up (Figures 7a–7d) and strengthen (supporting information Figures S1e–S1g) as f_{scale} increases. Although from this perspective it appears unlikely that a particular mode dominates the tail response, we acknowledge that a closer analysis of the association between extremes and variability would be needed to fully verify this, which is beyond the scope of this study. Meanwhile, we note the spectral responses are interesting in their own right. For instance, the Madden-Julian Oscillation (MJO) signals (eastward propagating oscillation with wavenumber of 1–2 and period of 30–60 days) are clearly visible in all simulations (Figures 7a–7d). PBD14 reported an insensitivity of SPCAM3's MJO signal across different CRM extent and throttling configurations. This new result now shows the MJO is intrinsically robust in SPCAM3 to both CRM extent and f_{scale}.

3.3. Comparison of Response With CAM3

Figure 8 reviews several additional climatologically important state variables, which helps to put the response of SPCAM3 to f_{scale} in the context of independent studies that have analyzed the effect of model time step on conventionally parameterized GCMs, including SPCAM3's twin sister, CAM3.0. All values shown in Figure 8 are the area-weighted horizontal average over tropical ocean (20°S–20°N).

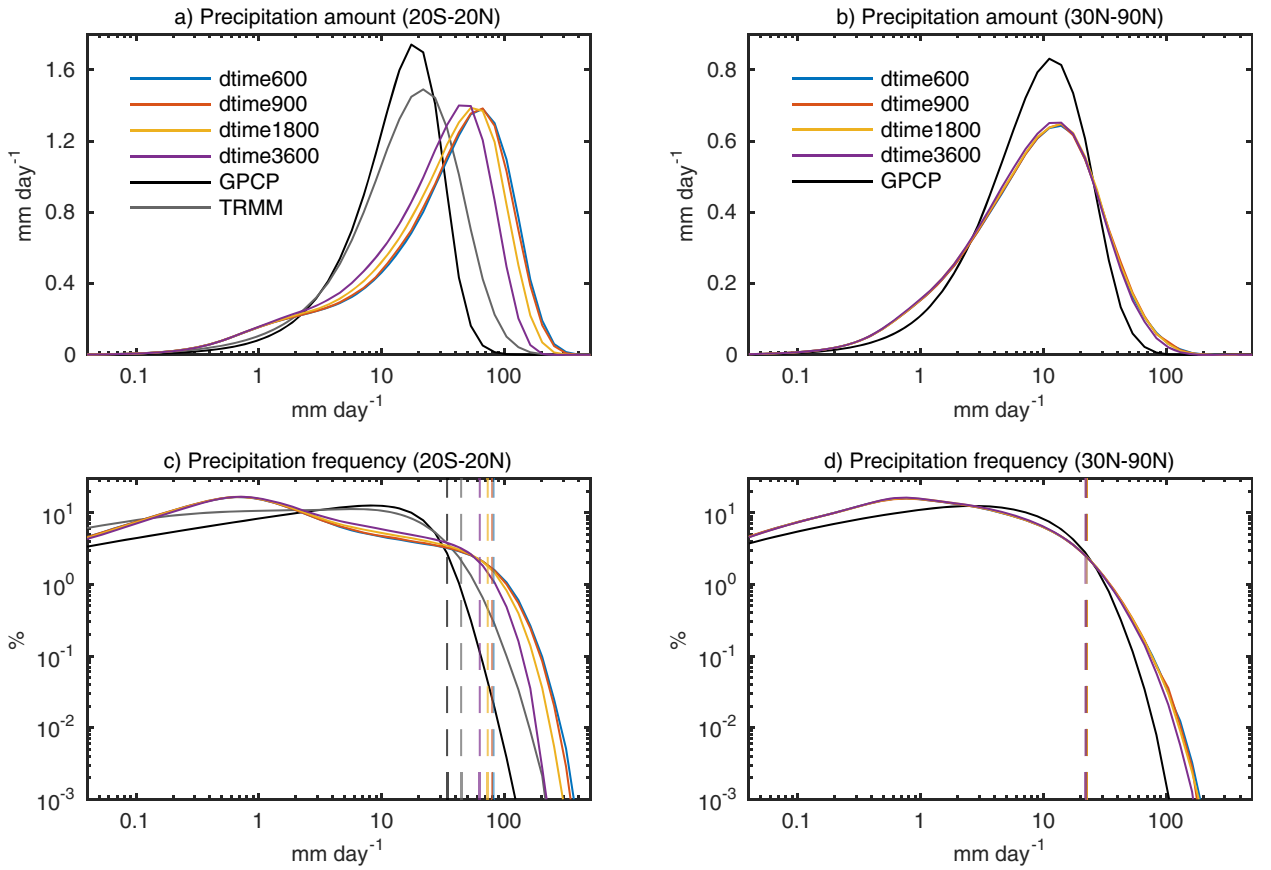

Figure 6. (top; a and b) Amount and (bottom; c and d) frequency distributions of daily mean precipitation rate in the (left; a and c) tropics (20°S–20°N) and (right; b and d) northern hemisphere extra tropics (30°N–90°N). Precipitation in southern hemisphere extra tropics (30°S–90°S) is very similar to b and d (not shown). The dashed lines in c and d show 99th percentiles of daily mean precipitation rate.

Tropical precipitable water (Figure 8a) decreases slightly with a higher f_{scale}. We emphasize that a drying of the column could be viewed as consistent with a shift to a more efficiently ventilated convective mixing state owing to less throttled convection at high f_{scale} (i.e., consistent with hypothesis H1). The drier near-surface layer is associated with slightly enhanced surface latent heat (LH) flux by 1–2 W/m^2 (Figure 8b), which is balanced through increased atmospheric moisture demand. That is, surface specific humidity anomaly responses to f_{scale} (Figure 8c) tend to mirror mean surface LH flux changes (Figure 8b) in the tropical horizontal average of surface LH flux as well as in its geographic pattern (not shown). In contrast, surface wind speed responses (Figure 8d) are inconsistent with the changes in surface evaporation.

It is logical to assess if any of these sensitivities are consistent to those of conventionally parameterized CAM3, since SPCAM3 shares many model components with CAM3. Below we review how our results compare with *Mishra and Sahany* [2011] (MS11 hereafter) who assessed the model time step sensitivity using CAM3 with a very similar model configuration to this study: real-geography, semi-Lagrangian dynamical core, T42 spectral resolution, 64 × 128 physical resolution. The tested time steps in MS11 were 300, 1200, and 3600 s.

Table 2 summarizes the sensitivities of important climate variables between SPCAM and CAM3 [MS11] in the wider tropics (30°S–30°N). The magnitude of sensitivity is measured as area-weighted, horizontally averaged, time-averaged value of the shortest time step (600 and 300 s) minus that of the longest time step (3600 and 3600 s) in each study (this study, MS11, respectively).

Interestingly, both time-mean SWCF and LWCF show *opposite* sensitivities in SPCAM3 and CAM3. The magnitudes of the SWCF sensitivity in both models are similar, but the LWCF sensitivity in SPCAM3 is much stronger (∼4×) than that in CAM3.

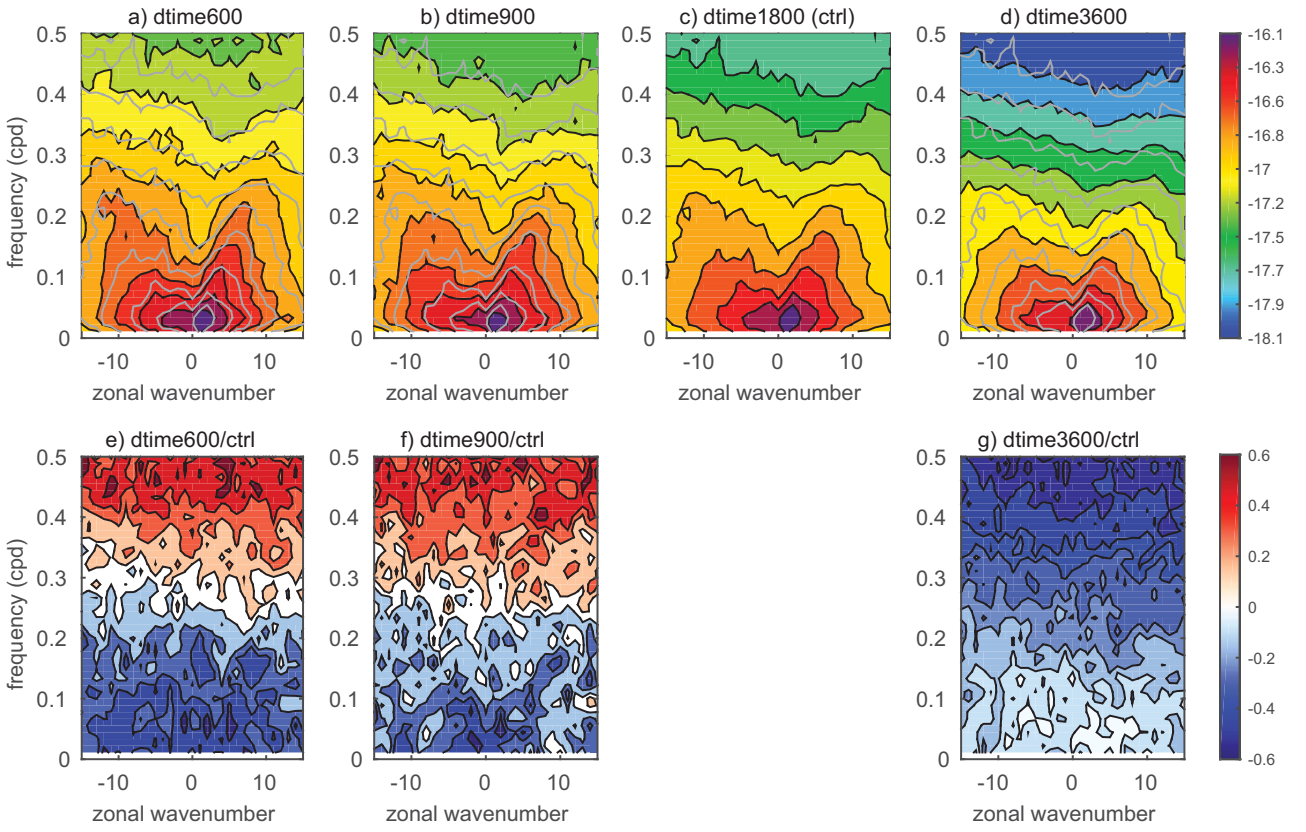

Figure 7. Zonal wavenumber-frequency log power spectra of equatorially symmetric daily mean precipitation rate in 10°S–10°N. (a–d) Raw log power spectra and (e–g) the ratio of log power of experimental simulation to control simulation. Gray contour lines in Figures 7a, 7b, and 7d are the contour line in the control simulation in Figure 7c.

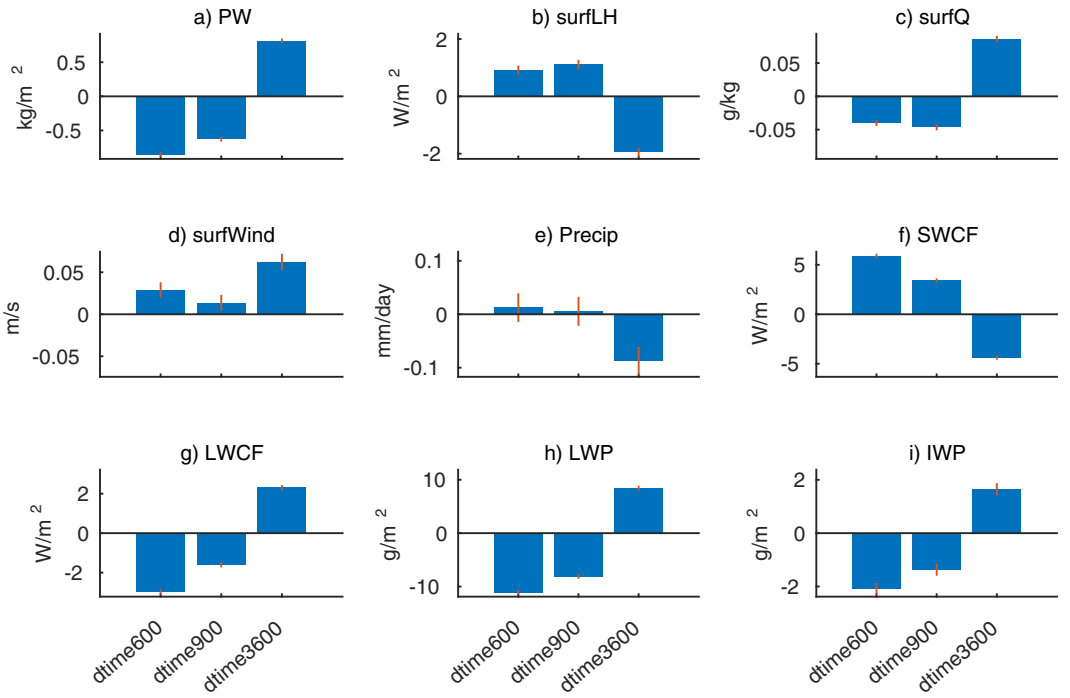

Figure 8. Area-weighted, annual mean anomalies of important climate variables over the tropical ocean (20°S–20°N). (a) Precipitable water, (b) surface latent heat flux, (c) surface specific humidity, (d) surface wind speed, (e) precipitation rate, (f) shortwave cloud forcing, (g) long-wave cloud forcing, (h) liquid water path, and (i) ice water path. The red error bars show 95% confidence intervals of monthly mean values.

Table 2. Comparison of Tropical (30°S–30°N) Mean Climate Sensitivities Between SPCAM3 and CAM3 When Global Model Time Steps Decrease[a]

	SPCAM3	CAM3
Shortwave cloud forcing	**Decrease (8.2 W/m^2)**	**Increase (10 W/m^2)**
Longwave cloud forcing	**Decrease (4.2 W/m^2)**	**Increase (1 W/m^2)**
Precipitation	Increase (0.1 mm/d)	Increase (0.1 mm/d)
precipitation intensity tail	Increase	Increase[b]
Precipitable water	Decrease (1.2 kg/m^2)	Increase (1.1 kg/m^2)
Surface evaporation	Increase (0.1 mm/d)	Increase (0.1 mm/d)
Surface specific humidity	Decrease (0.1 g/kg)	Decrease (0.1 g/kg)
Surface wind	Not systematic	Increase (0.05 or 0.2 m/s)
Moist Kelvin wave modes	Strengthen	Weaken
Equatorial wave modes at high frequency	Increase	Decrease[b]

[a]All variables are area-weighted, time-mean, and horizontally averaged first and then subtracted $\Delta t = 3600$ s ($\Delta t = 3600$ s) case from $\Delta t = 600$ s ($\Delta t = 300$ s) case for SPCAM3 (CAM3). CAM3 data are inferred from Figures 1 and 15 of *Mishra and Sahany* [2011]. Except cumulus parameterization, both simulation sets are done in very similar configurations: semi-Lagrangian dynamical core with T42 resolution, 10 year long, and real-geography. Major responses found in this study are marked in bold.

[b]More noticeable in aqua-planet CAM3 simulations in *Williamson* [2008].

The tropical mean precipitation is fairly insensitive to decreasing model time step in both models (consistent ~0.1 mm/d increase), but heavy precipitation frequency shows a noticeable sensitivity in both SPCAM3 and CAM3. In both models, the heavy precipitation events become more frequent as model time step decreases. Similar sensitivity is found also in aqua-planet CAM3 and CAM4 by *Williamson* [2008, 2013], respectively, that have argued the contributor of the heavy precipitation tail response is due to large-scale precipitation, not convective precipitation. The large-scale precipitation response seems to be attributed to the limited moist instability removal capability of cumulus parameterization suites in CAM3 and CAM4 with rigid convective instability depletion timescales [*Williamson*, 2013] as mentioned in section 1. We point out that this is unlikely to be the cause of the consistently signed precipitation tail response to f_{scale} in SPCAM3, since one would expect resolved CRM convection to efficiently remove convective instabilities as they develop. Nonetheless the precipitation tail response occurs in a consistent direction in both model types. (Refer to *DeMott et al.* [2007] for more in-depth comparison of precipitation variability between SPCAM3 and CAM3).

The equatorial wave responses to model time step are vastly different between SPCAM3 and CAM3. The first-order response to decreased time step in SPCAM3 is the shift of spectral power toward higher frequencies at all zonal wavelengths. In addition, the potential strengthening and propagation speed increase of moist Kelvin wave (MKW) modes are observed in SPCAM3. However, CAM3 shows very different responses. MS11 reported the decrease of spectral power at high-frequency, high-zonal wavenumber domain with a decreased time step in CAM3, but the systematic spectral power shift was unseen. MS11 also showed weakened spectral power and decreased propagation speed of MKW modes with a decreased time step in CAM3.

Interestingly, several SPCAM3 sensitivities to increasing exterior model *time resolution* show remarkable similarities to CAM3 sensitivities to increasing *horizontal resolution*. *Williamson* [2008] assesses the sensitivities of both time step and horizontal resolution in aqua-planet CAM3. While the time step sensitivity found in aqua-planet CAM3 are mostly consistent to MS11, a few variables exhibited sensitivities to horizontal resolution opposite to that in time step. For example, with increasing horizontal resolution at a fixed time step, precipitable water decreases, and the spectral power of tropical waves increases at high frequencies at all zonal wavelengths.

In summary, SPCAM3 and CAM3 show some key differences in their responses to global model time step. Time-mean shortwave cloud optical thickness is reduced in SPCAM3 but is oppositely increased in CAM3 as model time step is reduced. Secondary longwave cloud forcing responses are noticeable in SPCAM3 whereas they are mostly insignificant in CAM3. Although the tropical precipitation tail is increased in both models, there are inconsistent responses in the equatorial wave spectra. This confirms the effect of global model time step, perhaps through its additional effect of acting as a scale coupling frequency, can affect simulated climate in SP models in unique and unfamiliar ways.

3.4. Inconsistency With Throttling Expectations

Our null hypothesis (H0) is that SPCAM3 would be *insensitive* to f_{scale} due to the lack of rigid convective adjustment timescales that have been implicated in primary responses to model time step seen in conventionally parameterized GCMs. This is clearly ruled out—our findings show that the simulated climate in

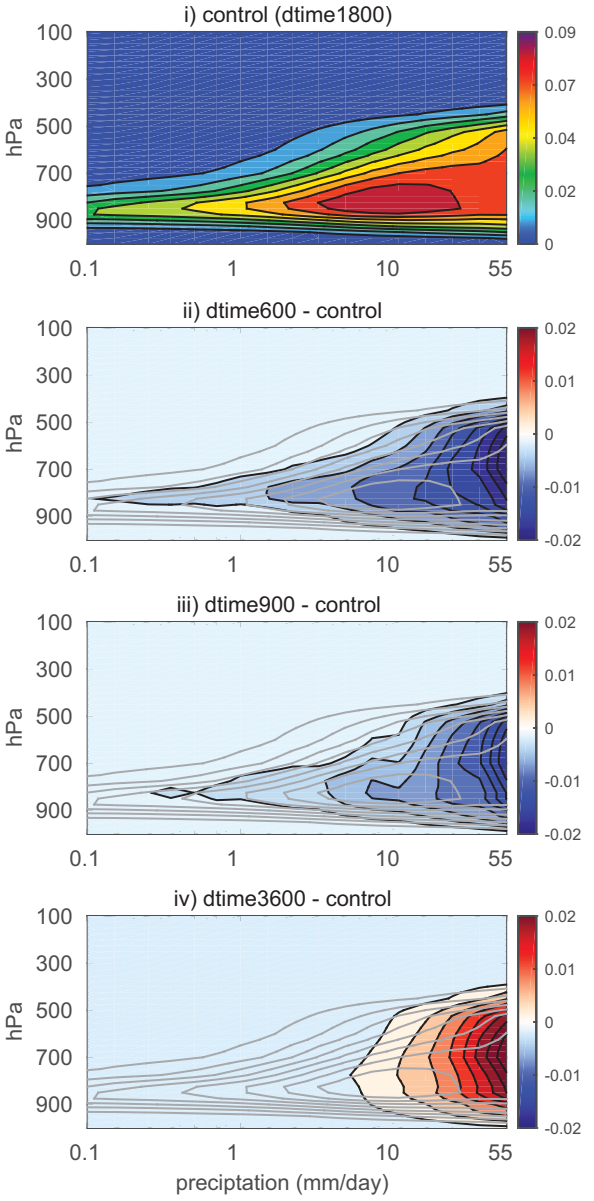

Figure 9. The daily precipitation-binned mean liquid condensate profile in an active convective region over ocean, 10°S–10°N, 60°E–170°E. (i) Control simulation and (ii–iv) experiment simulation anomalies against control simulation. The gray contour lines in Figures 9ii–9iv show the control simulation contour line in Figure 9i.

SPCAM3 is sensitive to f_{scale} at a comparable magnitude of time step sensitivities of CAM3, though in a different way.

Our alternative hypothesis (H1) is that f_{scale} might affect SPCAM's climatology through its effects on convective throttling physics in limited CRM domains. The expectation of H1 is that we would observe *reverse sensitivities* with increasing f_{scale} compared to those seen for reducing CRM domain extent in PBD14. The overall idea is that the artificial environment of locally trapped compensating subsidence inside a CRM is only formally true for a closed system within the timescale of a single GCM time step—such that if the GCM and CRM couple more frequently, biases imposed by a limited CRM domain size will be buffered by more frequent information exchange with large-scale dynamics. In other words, more frequent scale coupling could be viewed as a way to help "open" the artificially closed CRM system somewhat to compensate for artificial effects on mixing due to a limited CRM domain.

Consistent with the expectation from H1, increased f_{scale} has produced a striking effect reminiscent of lessened convective throttling—a monotonic reduction of SWCF biases in regions of the deepest convective mixing. Figure 9 confirms the systematic nature of this dominant response by analyzing the daily precipitation-binned, time-mean liquid condensate profile in an active convective region over ocean, 10°S–10°N, 60°E–170°E. This further emphasizes that the liquid condensate levels in the lower atmosphere systematically decrease *across all precipitation regimes* as f_{scale} increases. Consistent with H1, the reverse is seen in PBD14 (their Figure 12).

However, other aspects of the response to f_{scale} are inconsistent with an overarching convective throttling argument. For instance, the CRM-diagnosed net updraft mass flux profiles in tropical convective regions (Figure 10a) indicate that f_{scale} acts to *vertically shift* them toward a more bottom-heavy state—rather than *boosting* the magnitude of net saturated updraft mass fluxes throttled at all levels (the hallmark of the convective throttling mechanism; Figure 10b). This seriously undermines the credibility of the convective throttling hypothesis (H1). Distinctly, f_{scale} appears to affect the diabatic heating profile of convection rather than its mixing efficiency, with a higher f_{scale} promoting more bottom-heavy convection.

Other deeper lines of analysis further reveal inconsistencies with H1. For instance, the liquid water response to f_{scale} is a monotonic decrease at all vertical levels with a higher f_{scale} (Figure 9), while unwinding convective throttling is expected to cause a shift of condensate from lower to upper troposphere as shown in PBD14 (their Figure 12). Furthermore, H1 predicts the most extreme precipitation events should become less frequent with a higher f_{scale}. However, we have seen the reverse response in that the precipitation intensity tail boosts with a

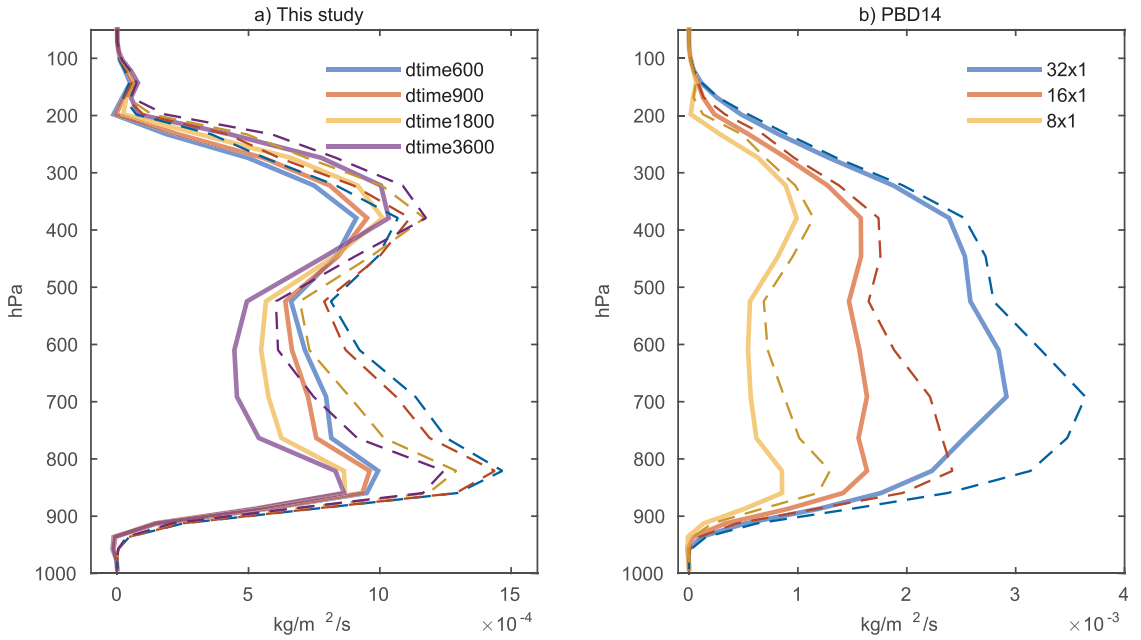

Figure 10. The profiles of the CRM-diagnosed updraft mass flux—the sum of saturated and unsaturated updraft mass flux components—(solid lines) and their saturated moist components (dashed lines) in (a) this study and (b) PBD14 in tropical convective regions (mean daily precipitation rate >6 mm/d in 15°S–15°N). Note the different scales on the abscissae in Figures 10a and 10b.

higher f_{scale} (Figure 6). Likewise, H1 predicts a vertical redistribution of convective heating with increased f_{scale} with unthrottling leading to more (less) convective energization at upper (lower) troposphere, another hallmark of planetary boundary layer ventilation effects not shown in PBD14 but shown in Figure 11b. However, this effect is not seen in the vertical profiles of moist static energy (MSE) tendency (Figure 11a). A weak sensitivity of the convective MSE tendency to f_{scale} is observed in the low atmosphere, but it is unlikely to be associated with convective moistening—i.e. the MSE tendency sensitivity is remarkably insensitive compared to the ventilation effects involving vertical redistribution under convective throttling in PBD14 (Figure 11b).

In short, there is convincing evidence that convective throttling arguments (H1) cannot explain the effect of f_{scale}.

3.5. Consequences of a Convective Organization Sensitivity

The above analysis has revealed that f_{scale} seems to produce a fundamental shift in the nature of *convective organization* (in terms of the vertical profile of convective mass fluxes and associated diabatic heating) in SPCAM3, with a reduced global model time step leading to more bottom-heavy convection. Here we explore whether an overarching argument beginning with a shift in the vertical structure of convection can explain the set of effects we have seen.

Figure 10a clearly shows the mass flux profile becomes more bottom-heavy as f_{scale} increases. Gross moist stability (GMS) is a useful metric here because it tells how efficiently column MSE is exported by horizontal divergence compared to the convective strength in a column, with clear links to the sensitivity of precipitation to external perturbations. We note that a more bottom-heavy mass flux profile would in turn import more MSE to a column because the environmental MSE decreases (increases) with height in lower (upper) troposphere. We follow *Raymond et al.* [2009] and normalize GMS by column vapor import but note that our conclusions are robust to alternately normalizing by dry static energy export as the measure of convective activity in the denominator of the normalized GMS, which is given by

$$GMS = -\frac{\int \nabla \cdot (h\mathbf{v})dp}{\int L_v \nabla \cdot (q\mathbf{v})dp}, \tag{1}$$

where h is the moist static energy, $\mathbf{v}$ is the horizontal velocity field, L_v is the specific latent heat of vaporization, and q is the specific humidity. The total advective tendencies of h and q are derived directly from the

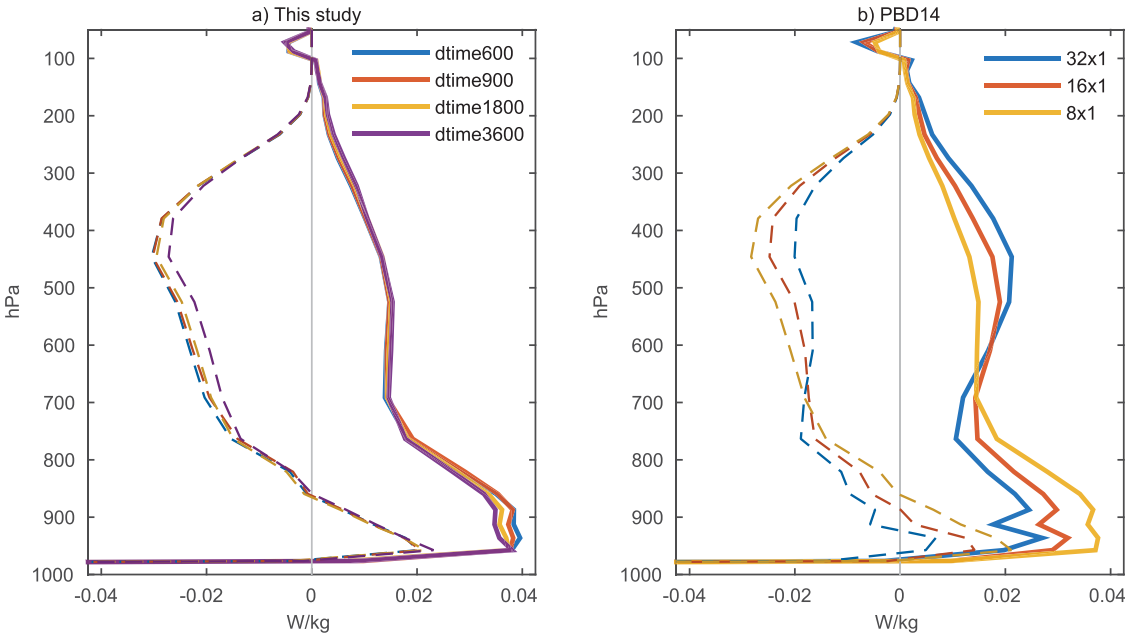

Figure 11. The profiles of the CRM-diagnosed MSE tendency—i.e., $c_p(\partial T/\partial t)+L_v(\partial q/\partial t)$, where T, q, c_p, and L_v are temperature, specific humidity, the specific heat capacity of air, and the specific latent heat of vaporization of water, respectively—(solid lines) and their moist components (dashed lines) in (a) this study and (b) PBD14 in tropical convective regions (mean daily precipitation rate >6 mm/d in 15°S–15°N).

model as the residual between the total tracked tendencies from daily model snapshots minus the daily mean accumulated tendency due to all model physics.

Figure 12 shows that time-mean GMS decreases with increased f_{scale} in active convective regions, as expected as a consequence of a more bottom-heavy profile of vertical mass flux. In addition, with a higher f_{scale}, the MSE profile becomes slightly steeper (i.e., more negative $\partial\theta_e/\partial z$) in the lower troposphere while the moist lapse rate does not change in the upper troposphere (not shown); this also contributes to the reduction of GMS as f_{scale} increases, but it is secondary to the vertical mass flux profile shifts. This GMS response is relevant to understanding the precipitation responses to f_{scale} because GMS defines a linkage between net precipitation (precipitation minus evaporation) and diabatic column MSE sources and sinks such as surface flux and radiative cooling (e.g., see Equations (2.1)–(2.3) in *Raymond et al.* [2009]). At steady state, a consequence of reduced GMS is enhanced sensitivity of net precipitation to a given magnitude of diabatic forcing of the column. From this view, the shift to a more bottom-heavy convective mass flux profile is consistent with an increased frequency of extreme rainfall events at high f_{scale}. Thus a change in tropics-wide vertical structure of convection may partially explain the tail response seen in the precipitation distribution. Similar arguments apply to precipitation variability, except that in unsteady cases it is possible that MSE storage in a column can also vary through moisture convergence which may modify the sensitivity of the precipitation to diabatic forcing.

The systematic reduction of SWCF and LWCF with increasing f_{scale} could be viewed as stemming from an overarching effect of convective organization resulting in increased precipitation efficiency (S. Tulich, personal communication). Thus organization changes could be viewed as an indirect cause of reduced column-integrated liquid water and ice water, and hence reduced shortwave and longwave cloud forcings. Indeed, the precipitation distribution shift toward more intense events could be a signal of increased precipitation efficiency, although a detailed analysis of condensation rates against surface precipitation would be needed to confirm this.

In summary, although impossible to explain with the convective throttling arguments under our original working hypothesis (H1), it seems possible to explain a broad set of responses to f_{scale} in SPCAM3 as the result of an overarching change in convective organization favoring more bottom-heavy convection, reduced gross moist stability, and enhanced precipitation efficiency at a high f_{scale}.

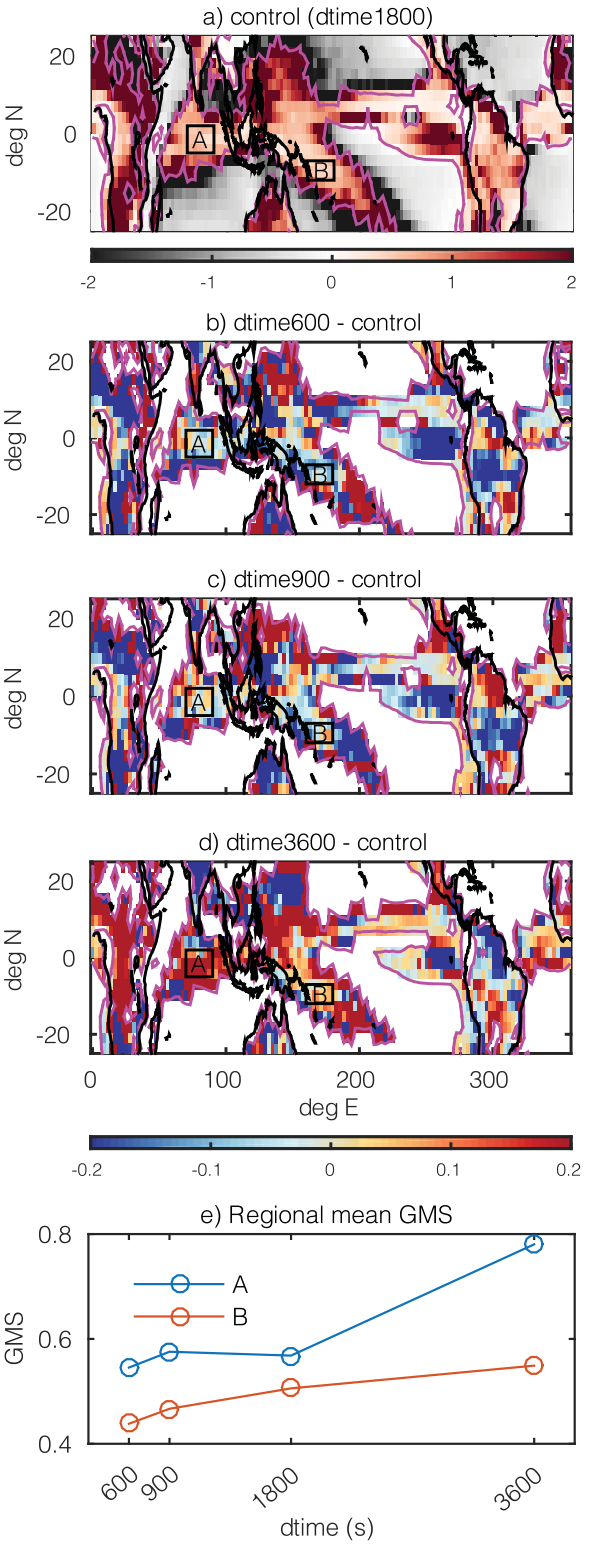

Figure 12. Annual mean normalized gross moist stability (GMS). (a) Control simulation, (b–d) experimental simulation anomalies against control simulation, and (e) horizontally averaged GMS responses in two indicated subregions A and B. The magenta line shows the contour of GMS of 0.1.

4. Discussion

It is unknown but worth speculating on what physical mechanisms might require an increasingly bottom-heavy convective profile as a result of a shorter global model time step (more frequent scale coupling between explicit deep convection and large-scale dynamics) in SPCAM3.

4.1. A Convection-Gravity Wave Feedback Strawman

We propose that a relevant mechanism could be enhancement in the efficiency of a known feedback between explicit convection and large planetary waves that leads to changes in bottom-heaviness in reduced-order simulations. *Kuang* [2011] (K11 hereafter) used a cloud system resolving model coupled instantaneously to advection from a single zonal gravity wave to explore the interaction between local convection and planetary-scale gravity waves. This dynamical scaffold can be viewed as an analog to SPGCMs—like SPCAM3, the K11 model explicitly resolves deep convection using a CRM, but within a simpler single-wave dynamical scaffold. The K11 model also enforces "stiff" (instantaneous) coupling to a single tropical gravity wave at a fixed wavelength whereas in SPCAM3 the coupling can be "loose" (infrequent, as limited by f_{scale}) and is with a spectrum of large-scale modes including but not limited to large tropical gravity waves.

Although indirect, the analogy is worth considering because K11 showed that when convection is allowed to feedback instantly with very large-scale gravity waves, top-heavy forms of convective organization become limited due to an intrinsic inconsistency with the large thermal anomalies that would be needed to balance them—tangentially, for our purposes, implying a breakdown of strict weak-temperature-gradient (WTG) [*Sobel et al.*, 2001] at sufficiently large zonal scales. It is conceivable that a similar organization-limiting mechanism could operate in SPCAM3 whereby increasing f_{scale} allows convection to feedback more "stiffly" (instantaneously) with GCM-resolved waves, including some that are large, and thus following reasons in K11 requiring a downward shift toward a more bottom-heavy form of organization. In contrast at a low f_{scale},

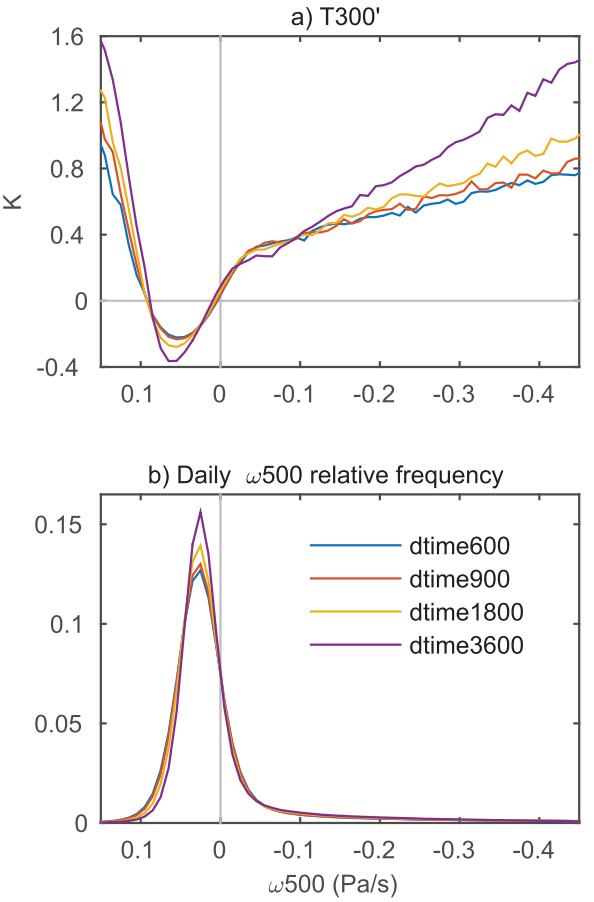

Figure 13. (a) Daily horizontal-mean anomalies of temperature from its horizontal field at 300 hPa ($T300'$) across vertical velocity at 500 hPa (ω 500) in equatorial region (5°S–5°N). (b) Relative frequency of vertical velocity at 500 hPa.

convection is left to its own devices for long periods, with infrequent and thus inefficient self-correcting large-scale gravity wave interaction. In this way, convection might become artificially top-heavy—that is, less bottom-heavy than it would have been interacting more frequently with a spectrum of waves, some of which are large.

The argument above is clearly speculative and we simply suggest it as a strawman for future work to either confirm or deny. It is not immediately obvious how to test it diagnostically in our simulations. Although it is tempting to causatively interpret thermal perturbations from the WTG on large zonal scales, since these are involved in the mechanisms that act to limit top-heaviness in the K11 analogy, this is not actually clear. On the one hand, one might expect increased departures from the WTG under high f_{scale} as a prediction from the analogy. But this need not be the case if thermal anomalies are part of self-limiting inconsistency that ultimately selects for a downward vertical shift to avoid excessive wave-interactive thermal anomalies. Thus it is difficult to derive insight on the validity of the analogy from diagnosis of free tropospheric temperature perturbations.

4.2. Weak-Temperature-Gradient Sensitivities

We nonetheless perform an analysis of the degree of departure from the WTG in our simulations, since it turns out to be interesting in its own right. Figure 13a shows the horizontally averaged daily temperature anomaly from the 5°S–5°N tropics-wide horizontal mean at 300 hPa ($T300'$). Under perfect WTG, these anomalies would be perfectly zero, but deviations can occur, and are found to be sensitive to f_{scale} in this study. To discriminate days and regions that are experiencing mean uplift from those that are subsiding, the results are further binned by the vertical velocity anomaly at 500 hPa (ω 500).

The interesting point in Figure 13a is that increasing f_{scale} reduces the magnitude of the $T300'$ such that SPCAM3's behavior becomes more WTG-like as f_{scale} increases. A vertically resolved view of this departure from the WTG (Figure 14) in tandem with the frequency distribution of midlevel ascent (Figure 13b) provides a suggestive clue to its cause (C. Bretherton, personal communication, 2015). The idea is that thermal anomalies arise from convective plumes as they deposit thermal energy by water vapor condensation in the upper atmosphere, but that these local heat anomalies (e.g., $T' > 0$) are then spread to adjacent GCM grid columns via dynamical adjustment. In SPGCMs, dynamical adjustment is limited by the timescale on which CRM and GCM are coupled. When longer time steps are used, local convection confined in an embedded CRM can build up to produce larger thermal anomalies that would in turn require a more vigorous GCM-scale vertical velocity response. This reasoning seems to satisfyingly explain both the increased magnitude of thermal departures from WTG when using longer time steps, as well as the transition to a more intense updraft spectrum in the $\omega < -0.1$ (Pa/s) range.

Of course this dynamical adjustment argument cannot explain the shift toward bottom-heavy mass flux profile, with an increased f_{scale}, that we have argued is an overarching cause of the set of climatological responses. But it is interesting to note that decreasing the global model time step reduces the

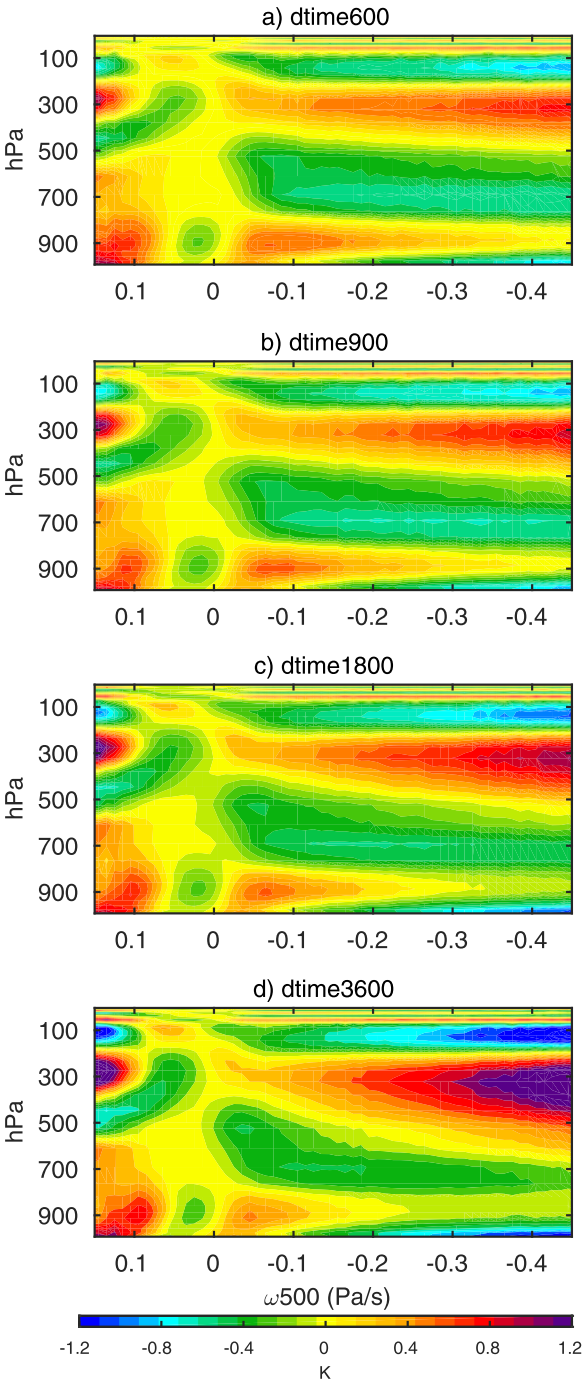

Figure 14. Vertically resolved profiles of temperature anomalies from its horizontal mean, binned by vertical velocity at 500 hPa (ω 500) in equatorial region (5°S–5°N).

magnitude of convectively induced horizontal thermal anomalies, effectively increasing the rigidity of the WTG in superparameterized simulations.

To further clarify which spatial scales produce the interesting effect of f_{scale} on WTG stiffness, we extend our analysis of $T'\omega$ to see its dependence on zonal wavelength. Figure 15 shows the zonal cospectrum between daily $T300'$ and ω 500 in the deep tropics (5°S–5°N). It suggests planetary-scale disturbances, i.e., small zonal wavenumbers, dominate the sensitivity to f_{scale} of the covariance between T' and ω. The overall sensitivity (weaker $T'\omega$ covariance with a higher f_{scale} in the small zonal wavenumber domain) is consistent with Figure 7, which shows the weakening of low-frequency equatorial waves—whose spectral power is most concentrated in small zonal wavenumbers—with increasing f_{scale}.

The fact that the very largest scales seem to respond especially to f_{scale} argues that more than local dynamic adjustment physics respond to f_{scale}. It is interesting to note that the largest scales are also those that were implicated in a shift to more bottom-heavy convection under "stiff" convection-gravity wave coupling in K11, though we acknowledge again that a direct linkage between our results and K11 is a bit unclear and worth further inquiry.

4.3. Is There an Optimal f_{scale}?

What should the global model time step/scale coupling frequency (f_{scale}) between CRM and GCM be set to in a perfect world?

Philosophically, it is tempting to think that infinitely fast scale coupling might be desirable for SP simulations such that individual updraft plumes can quickly interact with fast modes of large-scale dynamics such as GCM gravity waves. For instance, there could be multiple sequential deep convective plumes in a CRM domain within a given GCM time step. However, if f_{scale} is low, individual plumes are not able to interact with large-scale dynamics, e.g., exciting gravity waves or dynamic adjustment, because the scale coupling only passes the column-averaged information at the end of the CRM integration. In this line of thought, a higher f_{scale} is preferred in SPGCMs.

On the other hand, there are also good philosophical arguments to consider avoiding too frequent scale coupling (too short global model time step), based on the typical response timescales of CRM domain-mean properties being on the order of an hour or more, as well as unphysical intra-CRM effects (S. Tulich, personal communication, 2014). For instance, if f_{scale} is too high, a field of evolving cloud elements in a

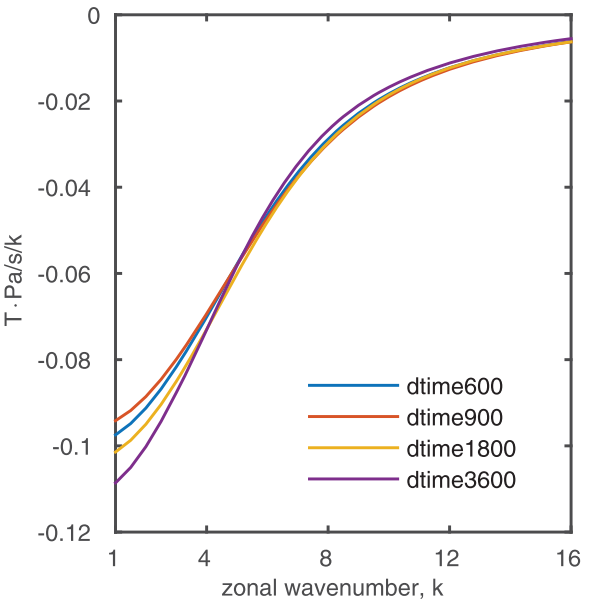

Figure 15. Cospectrum of daily temperature anomalies at 300 hPa and vertical velocity at 500 hPa from their horizontal field in equatorial region (5°S–5°N).

given CRM will not have had enough time to equilibrate with each other via mutual intra-CRM-scale gravity wave radiation, and portions of information can be prematurely transmitted between cloud elements through artificial interaction with the host GCM, which implicitly involves horizontal homogenization of information (see appendix in *Benedict and Randall* [2009] for further details on the CRM–GCM scaffold). In this line of thought, too high f_{scale} could be viewed as a philosophical problem for SP models that might produce artificially fast interaction between independent clouds inside CRMs. How or whether such artificial elements of the SP-scale interface engineering may have impacted problems seen in our and others' SPCAM simulations remains unclear but worth future inquiry.

Practically, some of our pilot-test results make a case for using very short global model time steps in superparameterized models. The favorable SWCF and LWCF responses and reduced tropical free tropospheric thermal anomalies might imply that an increased f_{scale} is better for SP simulations if time-mean cloud climatology and WTG-fidelity are key tuning factors. On the other hand, the trade-off of producing a very strong tropical extreme precipitation tail could be viewed as unsatisfying, although a stable estimate of the magnitude of this tail in observations is still in debate [*Liu and Allan*, 2012].

5. Conclusion

The effect of GCM time step (and hence scale coupling frequency f_{scale}) in the uncoupled SPCAM3 has been systematically assessed. A few important climate state variables are discovered to be systematically sensitive to f_{scale}. The most striking responses occur in time-mean cloud radiative forcing and appear to be promising: the zonally averaged annual SWCF and LWCF weaken and their biases against satellite observation are reduced at every latitude as f_{scale} increases. The magnitude of this sensitivity is most striking in SWCF ($\sim$10 W/m^2) and half as strong in LWCF ($\sim$5 W/m^2) in the tropics. That is, the climatology of low liquid clouds is more sensitive to f_{scale} than high clouds.

f_{scale} affects not only mean-state climate but also the tropical precipitation distribution. Extreme precipitation events become more frequent with increasing f_{scale}, which can exacerbate a preexisting precipitation bias in SPGCMs that use small, throttled CRMs for computational efficiency. It illustrates additional effects of f_{scale} can occur with trade-offs for climate simulation. This tail response is ubiquitous throughout the tropics and not significantly linked to any particular equatorial wave mode responses. Rather, the spectral power of tropical waves shifts toward higher frequencies at all zonal wavenumbers with increasing f_{scale}, although moist Kelvin wave modes show a weak mode-specific intensification.

The global model time step sensitivity of SPCAM3 is distinct from more familiar sensitivities that have been documented in the conventionally parameterized CAM. While both models show similar magnitude of sensitivities to time steps for the majority of compared variables, the signs of sensitivities of important climate variable disagree, including SWCF, LWCF, precipitable water, and the direction of spectral power shifts of equatorial waves. This discrepancy confirms model time step influences simulated climate of SPGCMs in a different way compared to traditional GCMs, possibly through their distinct role as the scale coupling frequency.

We began with a working hypothesis H1 that the dominant SWCF response may be the result of moist ventilation efficiency being modulated by f_{scale}. This builds on ideas of PBD14 that within a single GCM time

step, deep convective updrafts can become throttled by a limited CRM domain through overly strong compensating subsidence. In this context, a higher f_{scale} could play an important role in buffering artificial throttling by exposure to the large-scale dynamics of a host GCM. This view seemed consistent with the observed dominant response in our simulations of low-level liquid clouds decreasing monotonically with f_{scale}, especially in regions of strongest convection. However, it cannot explain other effects such as the LWCF bias reduction with increasing f_{scale}. More importantly, hypothesis H1 predicts the reverse expectation for the observed tropical precipitation tail response. It is also inconsistent with the observed vertical mass flux responses—the downward shift of the convective mass flux profile with increasing f_{scale}—which is distinct from the expectation of uniformly increased convective mass fluxes. Thus, contrary to our initial working hypothesis H1, our analysis revealed a higher f_{scale} does not unwind convective throttling and the SWCF responses are not the result of such unwinding, despite coincidentally similar geographic response signatures.

Instead, based on the balance of evidence, the primary effect of f_{scale} seems to induce a fundamental change in convective organization leading to a more bottom-heavy mass flux profile with a higher f_{scale}. Associated reduction of time-mean GMS might promote the intensification of heavy rainfall frequency in the tropics. From this view, enhanced precipitation efficiency associated with the new convective organization state could be viewed as ultimately driving the reduction of suspended condensate—and hence the systematic SWCF and LWCF responses and favorable reductions in cloud optical biases at a high f_{scale}.

It is unknown what fundamental physical processes ultimately respond to f_{scale} to require this systematic vertical shift in convective organization. We have speculated that the efficiency of convection-gravity wave feedbacks may play a role based on theoretical ideas put forward in K11 and consistent vertical shifts in SPCAM's convective mass fluxes. But we have emphasized it is difficult to causatively rule in or out. This topic would benefit from further inquiry and careful sensitivity study. The capabilities of the newly developed SP-WRF [*Tulich*, 2015] could prove especially illuminating in this regard, due to its unique ability to study superparameterization physics in limited domains and idealized configurations, with fully cloud-resolving benchmarks for validation. Work is underway using this new superparameterized model that illuminates a mechanism (S. Tulich, personal communication, 2015).

Meanwhile, the results of this study are already relevant to SPGCM simulations that take advantage of unusually small CRMs to gain some of the benefits of superparameterization without its full computational cost. SPGCM simulation is still computationally demanding despite the continuous expansion of computational resources. One way to make it more affordable is to use small CRMs, but this can distort mean climate, especially SWCF as shown in PBD14. Using higher f_{scale} can mildly alleviate this problem, though with trade-offs in the realism of tropical rainfall extremes and nature of convective organization. We note that using short global model time steps does not add much computational burden to an SPGCM because the number of CRM time steps is unchanged and the CRM workload dominates the SPGCM total computational workload. This is in contrast to conventional GCMs, where the global dynamics calculation tends to represent a nontrivial fraction of the overall computational workload, and thus calculating global dynamics more frequently can noticeably erode model's computational performance.

A limitation of this study has been the exclusive use of an unusually small CRM in all simulations, comprising only eight independent columns. While this had the advantage of starting from a highly throttled CRM configuration, designed to test a physical hypothesis, it may also have inadvertently stacked the decks for finding strong sensitivities to global model time step. Revisiting these sensitivity experiments in a baseline SPGCM using a CRM configuration with many more columns (32 or greater) would be helpful for testing the representativeness of some of our key findings. Such an analysis would require substantially more computational resources to investigate, and is beyond the scope of this study, but work on this front is underway.

Generally, there are several implications for understanding the emergent behavior of, and perhaps for tuning, the next generation of SPGCMs. SP models are relatively new and untuned, and the origins of some of their emergent convective organization, as well as their sensitivities to assumed scale coupling parameters, have not been fully assessed. The global model time step has proved to be an interestingly direct lever on the bottom-heaviness of simulated convection and the fidelity of the WTG, which may

help inform how the dynamics of organized convection manifest across the two resolved scales in SPGCMs. For tuning, although it does not fit the description in a traditional sense, f_{scale} could be regarded as a *dynamical* tuning parameter. In this context, its key eccentric property is to reversely affect the optical thickness of time-mean cloud fields versus the intensity of the tropical extreme rainfall tail. Whether these properties might prove to be useful ammunition for tuning, the next generation of SPGCMs depends on whether they can be leveraged against complementary trade-offs of other more traditional tuning parameters such as CRM microphysical assumptions. Such strategies could prove worth exploring as SPGCMs exit their infancy.

Acknowledgments
Funding for this study was provided by the Department of Energy under DE-SC0012152 and DE-SC0012548 and by the National Science Foundation (NSF) under AGS-1419518. Computational resources were provided by the Extreme Science and Engineering Discovery Environment, which is supported by NSF grant OCI-1053575, under allocation TG-ATM120034. We would like to thank Stefan Tulich, David Randall, and Robert Pincus for helpful comments. We would especially like to thank Brian Mapes for his original framing idea and Chris Bretherton for much insightful feedback. We gratefully acknowledge Gabriel Kooperman for providing analysis codes for precipitation distributions; Marat Khairoutdinov, David Randall, and Mark Branson for developing and distributing SPCAM 3.0 through CMMAP; and two anonymous reviewers for their comments that made this paper clearer. All simulation data in this study can be made available to scientific researchers upon request.

References

Benedict, J. J., and D. A. Randall (2009), Structure of the Madden-Julian Oscillation in the superparameterized CAM, *J. Atmos. Sci.*, *66*(11), 3277–3296.

DeMott, C. A., D. A. Randall, and M. Khairoutdinov (2007), Convective precipitation variability as a tool for general circulation model analysis, *J. Clim.*, *20*(1), 91–112.

Goswami, B. B., N. J. Mani, P. Mukhopadhyay, D. E. Waliser, J. J. Benedict, E. D. Maloney, M. Khairoutdinov, and B. N. Goswami (2011), Monsoon intraseasonal oscillations as simulated by the superparameterized Community Atmosphere Model, *J. Geophys. Res.*, *116*, D22104, doi:10.1029/2011JD015948.

Grabowski, W. W. (2001), Coupling cloud processes with the large-scale dynamics using the cloud-resolving convection parameterization (CRCP), *J. Atmos. Sci.*, *58*(9), 978–997.

Grabowski, W. W., and P. K. Smolarkiewicz (1999), CRCP: A cloud resolving convection parameterization for modeling the tropical convecting atmosphere, *Physica D*, *133*, 171–178.

Huffman, G. J., R. F. Adler, M. M. Morrissey, D. T. Bolvin, S. Curtis, R. Joyce, B. McGavock, and J. Susskind (2001), Global precipitation at one-degree daily resolution from multisatellite observations, *J. Hydrometeorol.*, *2*(1), 36–50.

Huffman, G. J., D. T. Bolvin, E. J. Nelkin, D. B. Wolff, R. F. Adler, G. Gu, Y. Hong, K. P. Bowman, and E. F. Stocker (2007), The TRMM Multisatellite Precipitation Analysis (TMPA): Quasi-global, multiyear, combined-sensor precipitation estimates at fine scales, *J. Hydrometeorol.*, *8*(1), 38–55.

Hurrell, J. W., J. J. Hack, D. Shea, J. M. Caron, and J. Rosinski (2008), A new sea surface temperature and sea ice boundary dataset for the community atmosphere model, *J. Clim.*, *21*(19), 5145–5153.

Khairoutdinov, M. F., and D. A. Randall (2003), Cloud resolving modeling of the ARM summer 1997 IOP: Model formulation, results, uncertainties, and sensitivities, *J. Atmos. Sci.*, *60*, 607–624.

Khairoutdinov, M., D. Randall, and C. DeMott (2005), Simulations of the atmospheric general circulation using a cloud-resolving model as a superparameterization of physical processes, *J. Atmos. Sci.*, *62*, 2136–2154.

Khairoutdinov, M., C. DeMott, and D. Randall (2008), Evaluation of the simulated interannual and subseasonal variability in an AMIP-style simulation using the CSU multiscale modeling framework, *J. Clim.*, *21*(3), 413–431.

Kuang, Z. (2011), The wavelength dependence of the gross moist stability and the scale selection in the instability of column-integrated moist static energy, *J. Atmos. Sci.*, *68*(1), 61–74.

Li, F., W. D. Collins, M. F. Wehner, D. L. Williamson, J. G. Olson, and C. Algieri (2011), Impact of horizontal resolution on simulation of precipitation extremes in an aqua-planet version of Community Atmospheric Model (CAM3), *Tellus, Ser. A*, *63*(5), 884–892.

Liu, C., and R. P. Allan (2012), Multisatellite observed responses of precipitation and its extremes to interannual climate variability, *J. Geophys. Res.*, *117*, D03101, doi:10.1029/2011JD016568.

Loeb, N. G., B. A. Wielicki, D. R. Doelling, G. L. Smith, D. F. Keyes, S. Kato, N. Manalo-Smith, and T. Wong (2009), Toward optimal closure of the earth's top-of-atmosphere radiation budget, *J. Clim.*, *22*(3), 748–766.

Mishra, S. K., and S. Sahany (2011), Effects of time step size on the simulation of tropical climate in NCAR-CAM3, *Clim. Dyn.*, *37*(3–4), 689–704.

Mishra, S. K., J. Srinivasan, and R. S. Nanjundiah (2008), The impact of the time step on the intensity of ITCZ in an aquaplanet GCM, *Mon. Weather Rev.*, *136*(11), 4077–4091.

Pendergrass, A. G., and D. L. Hartmann (2014a), Changes in the distribution of rain frequency and intensity in response to global warming, *J. Clim.*, *27*(22), 8372–8383.

Pendergrass, A. G., and D. L. Hartmann (2014b), Two modes of change of the distribution of rain, *J. Clim.*, *27*(22), 8357–8371.

Pritchard, M. S., M. W. Moncrieff, and R. C. J. Somerville (2011), Orogenic propagating precipitation systems over the United States in a global climate model with embedded explicit convection, *J. Atmos. Sci.*, *68*(8), 1821–1840.

Pritchard, M. S., C. S. Bretherton, and C. A. DeMott (2014), Restricting 32–128 km horizontal scales hardly affects the MJO in the superparameterized Community Atmosphere Model v. 3.0 but the number of cloud? Resolving grid columns constrains vertical mixing, *J. Adv. Model. Earth Syst.*, *6*, 723–739, doi:10.1002/2014MS000340.

Raymond, D. J., S. L. Sessions, A. H. Sobel, and Ž. Fuchs (2009), The mechanics of gross moist stability, *J. Adv. Model. Earth Syst.*, *1*, 9, doi:10.3894/JAMES.2009.1.9.

Rossow, W. B., A. Mekonnen, C. Pearl, and W. Goncalves (2013), Tropical precipitation extremes, *J. Clim.*, *26*(4), 1457–1466.

Sobel, A. H., J. Nilsson, and L. M. Polvani (2001), The weak temperature gradient approximation and balanced tropical moisture waves, *J. Atmos. Sci.*, *58*(23), 3650–3665.

Tan, M., A. Ibrahim, Z. Duan, A. Cracknell, and V. Chaplot (2015), Evaluation of six high-resolution satellite and ground-based precipitation products over Malaysia, *Remote Sens.*, *7*(2), 1504–1528.

Thayer-Calder, K., and D. A. Randall (2009), The role of convective moistening in the Madden-Julian Oscillation, *J. Atmos. Sci.*, *66*(11), 3297–3312.

Tulich, S. N. (2015), A strategy for representing the effects of convective momentum transport in multiscale models: Evaluation using a new superparameterized version of the Weather Research and Forecast model (SP-WRF), *J. Adv. Model. Earth Syst.*, *7*, 938–962, doi:10.1002/2014MS000417.

Wheeler, M., and G. N. Kiladis (1999), Convectively coupled equatorial waves: Analysis of clouds and temperature in the wavenumber-frequency domain, *J. Atmos. Sci.*, *56*(3), 374–399.

Williamson, D. L. (2008), Convergence of aqua-planet simulations with increasing resolution in the Community Atmospheric Model, Version 3, *Tellus, Ser. A*, *60*(5), 848–862.

Williamson, D. L. (2013), The effect of time steps and time-scales on parametrization suites, *Q. J. R. Meteorol. Soc.*, *139*(671), 548–560.

Williamson, D. L., and J. G. Olson (2003), Dependence of aqua-planet simulations on time step, *Q. J. R. Meteorol. Soc.*, *129*(591), 2049–2064.

Wolff, D. B., and B. L. Fisher (2009), Assessing the relative performance of microwave-based satellite rain-rate retrievals using TRMM ground validation data, *J. Appl. Meteorol. Climatol.*, *48*(6), 1069–1099.

Wyant, M. C., M. Khairoutdinov, and C. S. Bretherton (2006), Climate sensitivity and cloud response of a GCM with a superparameterization, *Geophys. Res. Lett.*, *33*, L06714, doi:10.1029/2005GL025464.